Communications in Physics, Vol. 31, No. 4 (2021), pp. 381-388
DOI:https://doi.org/10.15625/0868-3166/15927

DETECTION OF ULTRA-LOW CONCENTRATION OF METHYLENE BLUE BY POROUS SILICON PHOTONIC CRYSTALS COVERED WITH SIVER NANOPARTICLES AS EFFICIENT SERS SUBSTRATE

NGUYEN THUY VAN[1], VU DUC CHINH[1,2,†], PHAM THANH BINH[1,2], PHAM VAN HOI[1], BUI HUY[1], VU THI HONG HANH[3] AND PHAM VAN HAI[4]

[1]*Institute of Materials Science, Vietnam Academy of Science and Technology, 18 Hoang Quoc Viet, Cau Giay, Hanoi, Vietnam*

[2]*Graduate University of Science and Technology, Vietnam Academy of Science and Technology, 18 Hoang Quoc Viet Road, Cau Giay District, Hanoi, Vietnam*

[3]*Thai Nguyen University of Education, 20 Luong Ngoc Quyen Road, Thai Nguyen, Vietnam*

[4]*Hanoi National University of Education, 136 Xuan Thuy, Cau Giay, Hanoi, Vietnam*

E-mail: [†]chinhvd@ims.vast.vn

Received 10 March 2021
Accepted for publication 22 July 2021
Published 16 September 2021

Abstract. *In this work, porous silicon photonic crystals (PSi PhCs) covered by silver nanoparticles (AgNPs) were prepared as surface-enhanced Raman scattering (SERS) substrate to detect methylene blue (MB) at low concentrations. The limit of MB detection in water by the SERS substrate is evaluated to be 10^{-10} mol/L. The SERS signal intensities of 446 cm^{-1} and 1623 cm^{-1} peaks in SERS spectra of MB are fit in exponential functions of concentrations ranging from 10^{-4} to 10^{-10} mol/L. These results show that the AgNPs on PSi PhCs substrates could be applied in environmental sensing.*

Keywords: porous silicon; photonic crystal; silver nanoparticles; SERS; methylene blue.

Classification numbers: 42.55.Tv; 61.46.Df.

I. INTRODUCTION

Ultra-sensitive detection of trace amounts of chemicals has emerged due to the importance of environmental protection, biological detection and medical diagnosis. The surface-enhanced Raman scattering (SERS) is a powerful spectroscopic technique for ultrasensitive and selective bio-chemical detection [1–5], due to its capability of providing "fingerprint" of information of

molecular structures in low concentrations [6–8]. The enhancement mechanism of SERS has been explained by the highly local enhanced electromagnetic field on the noble metal surface due to the excitation of localized surface plasmon resonances and enhanced chemical interaction between the adsorbate and noble metal nanoparticles [9–11]. The local electromagnetic enhancement is much higher than the chemical enhancement [12–14]. The SERS substrates with many hot-spots and with uniform distribution of nanostructures on the surface have provided a large Raman enhancement and high repetition of measurement. Among the noble metals such as gold, silver, palladium, and platinum used normally in SERS substrates, the Ag nanostructure is considered to be one of the most excellent candidates for SERS application due to its highly desired plasmonic properties, low-cost and easy fabrication/synthesis.

Porous silicon photonic crystals (PSi PhCs) coated Ag nanoparticles (NPs) are shown to be as substrates for the improvement of SERS [15–18]. The enhancement of SERS depends on the localized surface plasmon resonance (LSPR) and the Raman polarizability. In PSi PhCs, interaction time of the light and matter increases by the multilayer structure. PhCs are lattices of thin films made of different dielectrics. Light is partially refracted, reflected, and transmitted at each interface. The lattice spacing, and the layer refractive indexes define whether the interference among reflected (or transmitted) beams is constructive (or destructive) at a specific wavelength and in turn, this defines the spectral region of the photonic band gap (PBG) [19]. The surface field distribution of photonic crystals is in a narrower region from the surface than that of single-layer films. In detail, the reflectance spectrum from the multi-layered PSi has a sharper reflectance area. When AgNPs are deposited on PSi PhCs, the enhanced electric field on the surface of PhCs is stronger, which leads to the enhancement of Raman optical signal. SERS activity of the substrates was tested using MB as the probe molecules. SERS on photonic crystal are much better than that on the single-layer structure substrates [17].

Methylene blue (MB) is a toxic organic substance which has been widely used in industry and pharmacy, which poses a threat to the environment and security due to its toxic properties. Methylene blue (MB, $C_{16}H_{18}ClN_3S$) is a reference agent [20–26] to confirm the capacity of SERS substrates at different concentrations. In this study, MB solution with different concentrations in bi-distilled water is used to investigate and evaluate the SERS activity.

In this paper, we propose the fabrication method for making SERS probe with Ag NPs on the PSi PhCs by using immersion plating process. The morphology of SERS substrates is characterized by field emission scanning electron microscope (FE-SEM). These results showed that growth and deposition of Ag nanostructures on the surface of PSi PhCs. The achieved SERS activity was experimentally demonstrated with the detection of low concentration of MB in aqueous solutions in the range from 10^{-4} to 10^{-10} M.

II. EXPERIMENT

II.1. Synthesis PSi PhCs substrates

PSi layers were produced by the electrochemical etching of p-type (100) silicon wafers with resistivity of $2 \div 4$ mΩ.cm in 13%–20% HF: ethanol solution. The electrochemical process was carried out without illumination. The process was computer-controlled, so precise control over current density and etching time was achieved, then it is resulting in a good control of the refractive index and thickness over the individual layers forming the multilayer systems. S-PSi

structures in this work were obtained with applied current density 50 mA/cm^2. PSi PhCs were formed by periodically varying the applied current density with two levels (J1 and J2) between 15 and 50 mA/cm^2. The number of periods for multilayer structures is 12. The multilayer has been rinsed in methanol and isopropanol after anodization and dried with nitrogen gas.

II.2. Preparation of SERS substrates

The synthesis and deposition of AgNPs on the PSi samples carriers out by following steps: The as-formed PSi samples that washed with deionized water and dried in air, were dipping into an ethanol solution of $AgNO_3$ with concentrations of 1 mM for immersion time as 1 minute at room temperature to synthesize AgNPs/PSi hybrid structures. Silver ions are reduced by hydrogen-silicon bonds in PSi.

II.3. Materials characterization and SERS measurement

The structure and morphology PSi PhCs and Ag NPs/PSi PhCs were examined by using FE-SEM, Hitachi S-4800, Japan. The reflectance spectra of PSi PhCs sample were performed on a spectrometer (USB-4000, Ocean Optics) and a halogen light source (HL-2000 Ocean Optics). Raman spectra were obtained by using Horiba Scientific LabRAM HR Evolution, with laser source of 785 nm light for excitation radiation. For each spectrum, the low laser power of 1.5 mW was used to avoid sample heating effects and the integration time was set as 10 s. The diameter of laser spot on sample surface is about 1 μm.

III. RESULTS AND DISCUSSION

IV. Morphological features of PSi PhCs

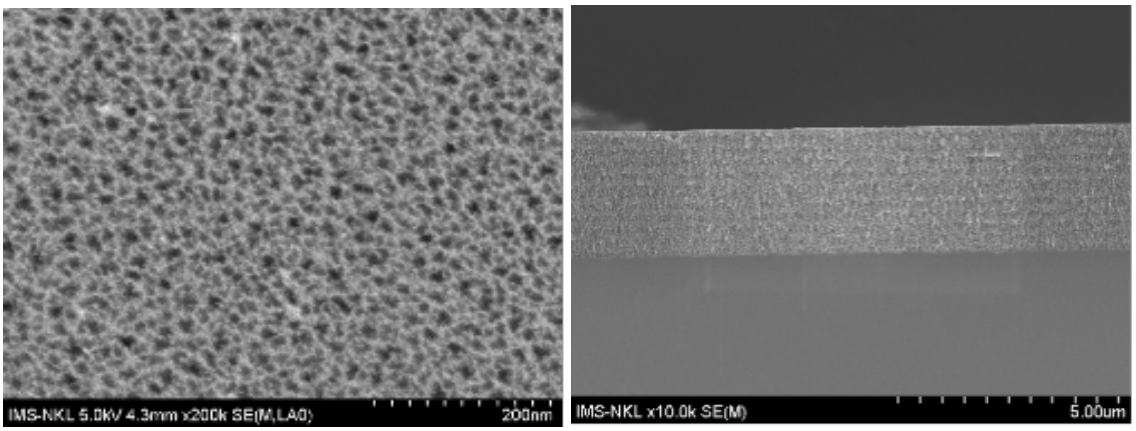

(a) (b)

Fig. 1. SEM images of PSi PhCs substrate: top view (a) and side view (b) of PSi.

The surface and side view of prepared PSi PhCs are shown in Figs. 1a and 1b, respectively. The pores in top view have the size of 20 nm which assist more Ag NPs to diffuse down into the Si pores. The side view showed hierarchy of 12 cycles and its thickness was ~ 2.9 μm. The

PSi PhCs nanostructure is obtained by periodically stacking two layers of a high (n_H) and low (n_L) refractive-index material, which has a thickness of λ/4, where λ is the central wavelength (λ is wavelength for fabrication of sample). From experimental results we calculated refractive indices of 2.1 and 1.75 for high- and low- refractive index layers, respectively. The influence of the number of periods on the reflectance spectrum has also been demonstrated in our previous publication [27] and the suitable number of periods is 12.

Figure 2 shows the SEM image of Ag NPs on PSi PhCs obtained. In general, Ag NPs with quasi- sphere shape were distributed rather uniformly over the surface. Their size ranges from 10 to 50 nm with an average size of 30 nm.

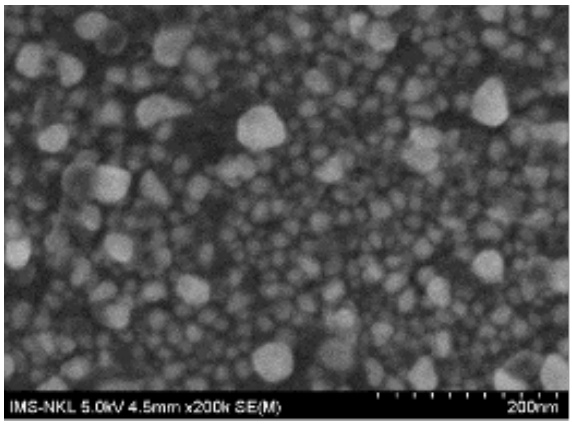

Fig. 2. SEM micrograph of silver layer deposited on PSi.

IV.1. Reflectance spectra

The reflectance spectrum of PSi PhCs is presented in Fig. 3. The wavelength range of the bandgap at 625-800 nm and a sharp peak at $\sim$ 785 nm were observed. It is expected to promote of high Raman scattering [28]. The reflectance spectrum of the PSi PhCs consists of a strong peak corresponding to the optical response of the photonic crystal [29].

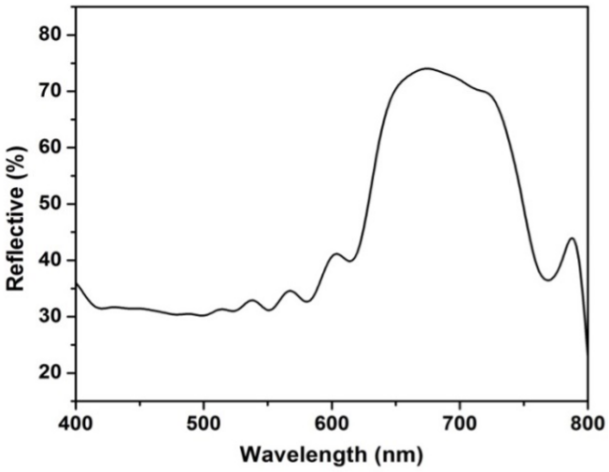

Fig. 3. Reflectance spectrum of the PSi PhC.

IV.2. The SERS activity of the substrates

Figure 4 shows the SERS spectra of MB at different concentrations on Ag NPs/PSi PhCs. An amount of 10 μL of each sample was dripped onto a silicon template for a SERS measurement. MB had Raman bands at $\sim$ 446 cm^{-1} and 1623 cm^{-1} that are attributed to the C–S–C skeletal deformation mode and C–C ring stretching, respectively. They are typical and most intense ones [21, 30–35]. The Raman spectra show a negligible weak signal at concentrations of 10^{-11} M and below. The Raman peaks at 446 cm^{-1} and 1623 cm^{-1} in Fig. 4 were evaluated, their intensity of the designated peak exponentially changes with the concentrations that are presented in Fig. 5. As shown in Fig. 5, within the concentration varying from 10^{-10} M to 10^{-4}M, the SERS intensity of both peaks changes exponentially according to the curve fitting equation $y = \exp(x + 12.57)$ and $y =$

$\exp(x+11.52)$ for 446 cm^{-1} and 1623 cm^{-1}, respectively. The peak at 520 cm^{-1} assigned to silicon wafer [35].

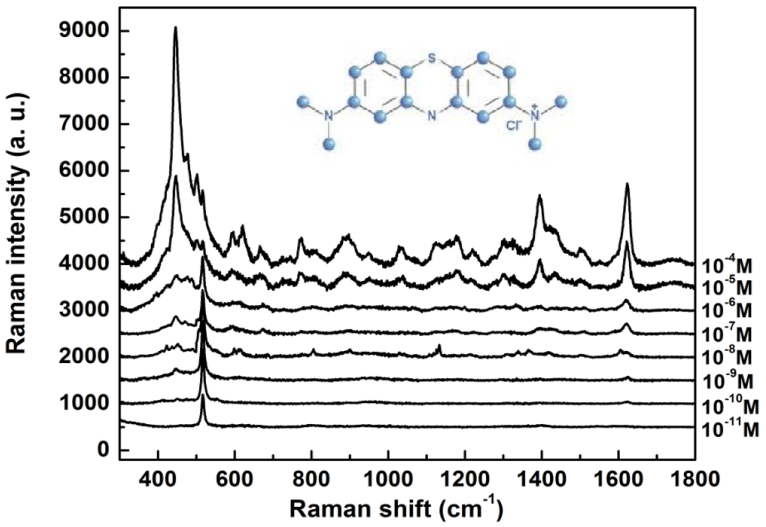

Fig. 4. SERS signals of MB with different concentration s rang eing from 10^{-11} to 10^{-4}M on the Ag NPs/PSi PhCs substrate.

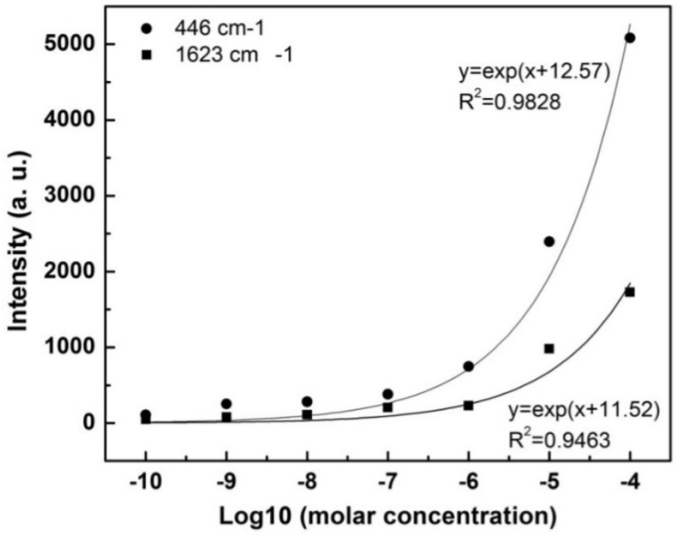

Fig. 5. Calibration curve of SERS intensity at 446 and 1623 cm^{-1}.

In this experiment, following the method of Han [36], silicon with a Raman peak at 520 cm^{-1}, was used as an internal standard to eliminate instrumental variables [37]. The intensity ratio of a strong peak at 446 cm^{-1} (and 1623 cm^{-1}) assigned to MB and a peak at 520 cm^{-1} assigned to

silicon (I_{446}/I_{520} and I_{1623}/I_{520}) was measured. As shown in Fig. 6, the increase of I_{446}/I_{520} and I_{1623}/I_{520} followed along with the increase of the MB concentration added into the SERS template. More important, the ratio of I_{446}/I_{520} increase d stronger than that of I_{1623}/I_{520}. From the changes in intensities of the bands on the SERS signal, we can deduce that MB adopts a parallel fashion to the silver colloid surface, and it tends to make S-Ag at the surface. Consequently, at higher MB concentration, the band at 446 cm^{-1} which is related to C-S-C skeletal deformation, enhanced a lot. This analysis has been rarely reported in other published papers.

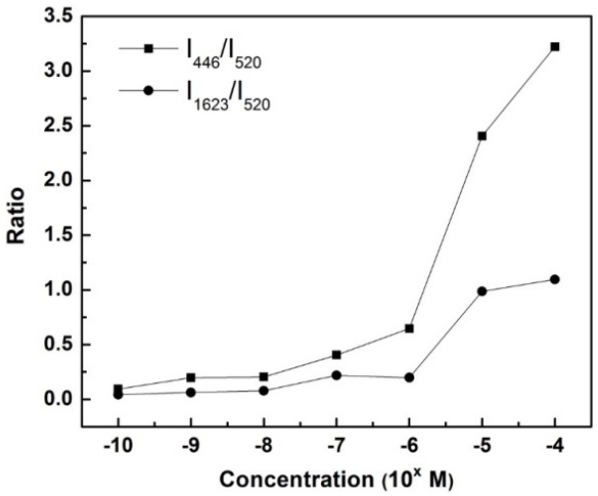

Fig. 6. SERS intensity ratio of 446 to 520 cm^{-1} (I_{446}/I_{520}) and 1623 to 520 cm^{-1} (I_{1623}/I_{520}) versus MB concentration.

To determine the role of silicon nanostructures in the Raman enhancement, the Raman spectra MB on Ag NPs/PSi PhCs and Ag NPs/s-PSi were compared. After MB molecules (10^{-7} M concentration) were adsorbed on these substrates, Raman spectra were measured and evaluated. All the Raman spectra were recorded under the same measuring conditions by an excitation laser at the wavelength of 785 nm and the power of 1.5 mW. As shown in Fig. 7, the Raman spectra obtained from those two samples are different. The SERS signal from MB adsorbed on Ag NPs/s-PSi was much smaller than that on Ag NPs/PSi PhCs. With Ag NPs/PSi PhCs, the Raman band of MB molecules at 446 cm^{-1} and 1623 cm^{-1} are 4.2 and 6.1 times stronger than that on Ag NPs/s-PSi, respectively. So, the role of PSi PhCs in the Raman enhancement dominates clearly. For the PSi PhCs nanostructure, the internal reflections in multilayers can enhance the Raman signals [38].

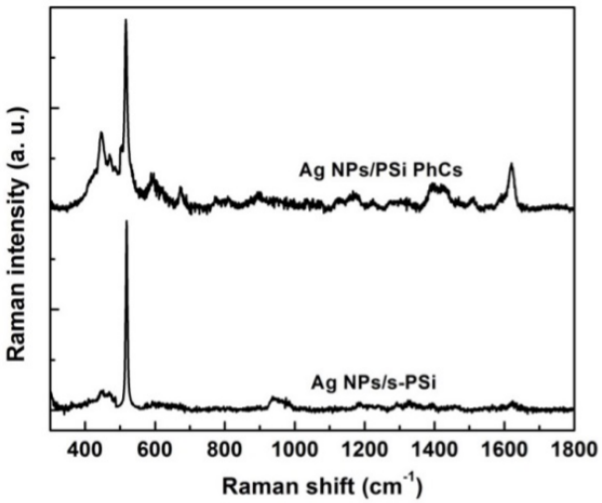

Fig. 7. The SERS spectra of MB molecules (10^{-7} M concentration) adsorbed on Ag NPs/s-PSi and Ag NPs/PSi PhCs substrate.

The enhancement of SERS depends on the localized surface plasma resonance (LSPR) of the obtained material and the enhancement of Raman polarizability that results from the increasing interaction time of the light and matter of the multilayer structure. The electric field on the photonic crystal surface is stronger than that on the single-layer film. The surface field distribution of photonic crystals is in a narrower region from the surface than that of single-layer films. Thus, Ag nanoparticles are deposited on the two types of porous silicon samples, the enhanced electric field on the surface of photonic crystals is conducive to achieving stronger the strong LSPR response, which leads to the enhancement of Raman optical signal.

V. CONCLUSIONS

In summary, we have successfully growth and deposited Ag NPs on the PSi PhCs by a facile technique. This SERS substrate can detect MB in distilled water with concentrations in the range of 10^{-10} M – 10^{-4} M. Its limit of detection (LOD) is 10^{-10} M. The SERS activity was sensitive to the different PSi morphology. The results indicated that the Raman signal on Ag NPs/PSi PhCs was higher ~ 5 times than that on Ag NPs/s-PSi. Higher sensitive SERS in Ag NPs/PSi PhCs is due to the light-wave modulation. Our result demonstrates that the nanostructures of Si effect strongly on the enhancement of SERS. Therefore, Ag NPs/PSi PhCs substrate could be a promising candidate for portative SERS equipment which can be used for rapid, real-time detection of chemical compounds in the liquid environment in outdoor fields.

ACKNOWLEDGMENT

This research is funded by Vietnam Academy of Science and Technology under grant number VAST 03.07/20-21; Vietnam National Foundation for Science and Technology Development (NAFOSTED) under grant number 103.03-2019.310.

REFERENCES

[1] B. S. Lee, P. C. Lin, D. Z. Lin and T. J. Yen, *Scientific Reports* **8** (2018) 516.
[2] J. Tang, M. Yu, T. Jiang, E. Wang, C. Ge and Z. Chen, *Optik* **136** (2018) 244.
[3] T. B. Pham, T. H. C. Hoang, V. H. Pham, V. C. Nguyen, T. V. Nguyen, D. C. Vu, V. H. Pham and H. Bui, *Scientific Reports* **9** (2019) 12590.
[4] T. B. Pham, V. C. Nguyen, V. H. Pham, H. Bui, R. Coisson, V. H. Pham and D. C. Vu, *Journal of Nanoscience and Nanotechnology* **20** (2020) 1928.
[5] R. P. Zaccaria, F. Bisio, G. Das, G. Maidecchi, M. Caminale, C. D. Vu, F. De Angelis, E. Di Fabrizio, A. Toma and M. Canepa, *ACS Appl. Mater. Interfaces* **8** (2016) 8024.
[6] Z. Zhu, V. W. Espulgar, H. Yoshikawa, M. Saito, B. Fan, X. Dou and E. E. Tamiya, *Bulletin of the Chemical Society of Japan* **91** (2018) 1579.
[7] C. Zong, M. Xu, J. L. Xu, T. Wei, X. Ma, S. X. Zheng, R. Hu and B. Ren, *Chemical Reviews* **118** (2018) 4946.
[8] Z. Yin, Y. Wang, C. Song, L. Zheng, N. Ma, X. Liu, S. Li, L. Lin, M. Li, Y. Xu, W. Li, G. Hu, Z. Fang and D. Ma, *Journal of the American Chemical Society* **140** (2018) 864.
[9] R. Wang, K. Kim, N. Choi, X. Wang, J. Lee, J. H. Joen, G. Rhie and J. Choo, *Sensor and Actuators B: Chemical* **270** (2018) 72.
[10] H. Zhang, Y. Kang, P. Liu, X. Tao, J. Pei, H. Li, and Y. Du, *Analytical Letters* **49** (2016) 2268.
[11] B. Han, Y. L. Zhang, L. Zhu, X. H. Chan, Z. C. Ma, X. L. Zhang, J. N. Wang, W. Wang, Y. Q. Liu, Q. D. Chen and H. B. Sun, *Sensor and Actuators B: Chemical* **270** (2018) 500.
[12] K. Wang, Y. Wang, C. Wang, X. Jia, J. Li, R. Xiao and S. Wang, *RSC Advances* **8** (2018) 30825.

[13] D. Cheng, M. He, J. Ran, G. Cai, J. Wu and X. Wang, *Sensor and Actuators B: Chemical* **270** (2018) 508–517.
[14] S. Jiang, J. Guo, C. Zhang, C. Li, M. Wang, Z. Li, S. Gao, P. Chen, H. Si, and S. Xu, *RSC Advances* **7** (2017) 5764.
[15] F. Zhong, Z. Wu, J. Guo and D. Jia, *Nanomaterials* **8** (2018) 872.
[16] H. V. Bandarenka, V. G. Kseniya, S. A. Zavatski, A. Panarin and S. N. Terekhov, *Materials* **11** (2018) 852.
[17] G. Lu, G. Wang, and H. Li, *RSC Adv.* **8** (2018) 6629.
[18] A. M. Alwan, L. A. Wali and A. A. Yousif, *Silicon* **10** (2018) 2241.
[19] P. Lova, G. Manfredi, and D. Comoretto, *Adv. Optical Mater.* **6** (2018) 1800730.
[20] E. N. Aybeke, Y. Lacroute, C. Elie-Caille, A. Bouhelier, E. Bourillot and E. Lesniewska, *Nanotechnology* **26** (2015) 245302.
[21] T. T. H. Pham, X. H. Vu, N. D. Dien, T. T. Trang, N. V. Truong, T. D. Thanh, P. M. Tan and N. X. Ca, *RSC Adv.* **10** (2020) 24577.
[22] G. Laurent, N. Felidj, J. Grand, J. Aubard, G. Levi, A. Hohenau, F. R. Aussenegg and J. R. Krenn, *Phys. Rev. B* **73** (2006) 245417.
[23] G-N. Xiao and S-Q. Man, *Chem. Phys. Lett.* **447** (2007) 305.
[24] A. Merlen, V. Gadenne, J. Romann, V. Chevallier, L. Patrone and J. C. Valmalette, *Nanotechnology* **20** (2009) 215705.
[25] X. Dong, H. Gu, J. Kang, X. Yuan and J. Wu, *J. Mol. Struct.* **984** (2010) 396.
[26] N. Nuntawong, M. Horprathum, P. Eiamchai, K. Wong-ek, V. Patthanasettakul and P. Chindaudom, *Vacuum* **84** (2010) 1415.
[27] B. Huy, P. V. Hoi, D. T. Chi, P. H. Khoi and N. T. Van, *Int. J. Nanotec hnol.* **8** (2011) 360.
[28] J. J. Wang, Z. H. Jia and Y. Liu, *IEEE Sensors Journal* **19** (2019) 11221.
[29] C. Pacholski, *Sensors (Basel)*. **13** (2013) 4694.
[30] R. R. Naujok, R. V. Duevel and R. M. Corn, *Langmuir* **9** (1993) 1771.
[31] K-D. Shim and E-S. Jang, Bull. *Korean Chem. Soc.* **39** (2018) 936.
[32] K. T. Tu and C. K. Chung, *Journal of The Electrochemical Society* **164** (2017) B3081.
[33] E. N. Aybeke, Y. Lacroute, C. Elie-Caille, A. Bouhelier, E. Bourillot and E. Lesniewska, *Nanotechnology* **26** (2015) 245302.
[34] M. Zannotti, A. Rossi and R. Giovannetti, *Coatings* **10** (2020) 288.
[35] X. Guo, Z. Guo, Y. Jin, Z. Liu, W. Zhang and D. Huang, *Microchim Acta* **178** (2012) 229.
[36] X. X. Han, Y. Xie, B. Zhao and Y. Ozaki, *Anal. Chem.* **82** (2010) 4325.

[37] S. E. J. Bell and N. M. S. Sirimuthu, *Chem. Soc. Rev.* **37** (2008) 1012.
[38] I. Alessandri, *J. Am. Chem. Soc.* **135** (2013) 5541.